

How periodic orbit bifurcations drive multiphoton ionization

S. Huang^{1,*}, C. Chandre², and T. Uzer¹

¹ Center for Nonlinear Science, School of Physics,

Georgia Institute of Technology, Atlanta, Georgia 30332-0430, U.S.A.

² Centre de Physique Théorique - CNRS, Luminy - Case 907, 13288 Marseille cedex 09, France

The multiphoton ionization of hydrogen by a strong bichromatic microwave field is a complex process prototypical for atomic control research. Periodic orbit analysis captures this complexity: Through the stability of periodic orbits we can match qualitatively the variation of experimental ionization rates with a control parameter, the relative phase between the two modes of the field. Moreover, an empirical formula reproduces quantum simulations to a high degree of accuracy. This quantitative agreement shows how short periodic orbits organize the dynamics in multiphoton ionization.

PACS numbers: 32.80.Rm, 05.45.-a

Simple systems can display extraordinarily complex dynamics: This lesson from three decades of chaos theory has altered the direction of many areas of physics [1]. One-electron systems, which are the most fundamental at the atomic level, have had their fair share of such striking new discoveries [2], a prominent example being the multiphoton ionization of hydrogen in a strong microwave field [3]. Its interpretation remained a puzzle until its stochastic, diffusional nature was uncovered through the then-new theory of chaos [4]. Feverish research activity in the last thirty or so years has resulted in a fairly complete understanding of this problem [5, 6, 7]. As in many other areas of physics, here too the emphasis has shifted lately from understanding the process to using those insights to manipulating it [8, 9]. Clearly, the hope is that experience gained from this prototypical system will help to control more complex systems ranging from atoms to plasmas. Here control denotes tailoring the physical behavior of nonlinear dynamical systems (which generically exhibit chaotic dynamics) using “knobs” (i.e., suitable external parameters). Success depends on identifying simple knobs and understanding why and how they alter the system. In this Letter we report on precisely such a knob for a complex quantum system, and show how ionization behavior can be predicted with quantitative accuracy using periodic orbits.

The ionization of a one-dimensional hydrogen atom driven by a bichromatic linearly polarized electric field is a seemingly simple set-up with complex dynamics. Bichromatic pulses [10, 11] have emerged as natural tools in atomic control research because the relative phase of the two phase-locked pulses offers a practical control knob [12, 13, 14, 15, 16, 17, 18, 19, 20, 21, 22]. The Hamiltonian of the system is, in atomic units,

$$H = \frac{p^2}{2} - \frac{1}{x} + F_h x \sin(h\omega t) + F_l x \sin(l\omega t + \phi), \quad (1)$$

where the indices l, h refer to the low and high frequency

modes with frequencies $l\omega$ and $h\omega$, respectively. These two modes are frequency locked, i.e. l and h are integers. They are out-of-phase by ϕ , the control parameter.

In what follows, we consider Hamiltonian (1) for the two sets of experimental parameters of Ref. [20]: (I) the $h:l=3:1$, $F_h = 24 \text{ Vcm}^{-1}$ and $F_l = 53.4 \text{ Vcm}^{-1}$, and (II) the $h:l=3:2$, $F_h = 25 \text{ Vcm}^{-1}$ and $F_l = 33.5 \text{ Vcm}^{-1}$. The highest frequency is 18 GHz in both cases. These two sets show experimentally and numerically drastically different ionization behavior [20] and in the frequency range considered, these results can be reproduced by quantum or classical simulations. Our purpose here is to show that these findings can be qualitatively and quantitatively captured using a periodic orbit analysis, which reveals the classical bifurcations responsible for ionization. It also allows prediction of ionization at other values of parameters without resorting to large numerical simulations.

We begin by mapping Hamiltonian (1) into action-angle variables such that the principal quantum number n is associated with action J . We assume $\omega = 1$ without loss of generality. Hamiltonian (1) becomes [5]

$$H = -\frac{1}{2J^2} + 2J^2[F_h \sin(ht) + F_l \sin(lt + \phi)] \left(a_0/2 + \sum_{k=1}^{\infty} a_k \cos k\theta \right), \quad (2)$$

where $a_n = [J_n(n) - J_{n-1}(n)]/n$ and J_n 's are Bessel functions of the first kind. Note that there are three variables (J, θ, t) and three parameters (F_h, F_l, ϕ). We denote this Hamiltonian $H(J, \theta, t; \phi)$ where (F_h, F_l) are chosen according to Cases (I) or (II).

For this Hamiltonian, we consider a specific periodic orbit, denoted $\mathcal{O}(0)$ for $\phi = 0$. Numerically it is determined using a modified Newton-Raphson multi-shooting algorithm as described in Ref. [1]. We follow this periodic orbit as ϕ is varied. The orbit $\mathcal{O}(0)$ deforms continuously into $\mathcal{O}(\phi)$, the period of which is denoted $T(\phi)$. In addition to its location, we also monitor its linear stability properties obtained from the reduced tangent flow ex-

*Electronic address: gtg098n@mail.gatech.edu

pressed as

$$\frac{d\mathcal{J}_\phi^t}{dt} = \mathbb{J}\nabla^2 H(J, \theta, t; \phi)\mathcal{J}_\phi^t,$$

where \mathbb{J} is the two-dimensional skew-symmetric matrix and $\nabla^2 H$ is the two-dimensional Hessian matrix (composed by second derivatives of H with respect to its canonical variables J and θ). The initial condition is $\mathcal{J}_\phi^0 = \mathbb{I}_2$ (the two-dimensional identity matrix). The stability properties are given by the two eigenvalues of the monodromy matrix $\mathcal{J}_\phi^{T(\phi)}$ which form a pair $(\lambda, 1/\lambda)$ (since the flow is volume preserving, the determinant of $\mathcal{J}_\phi^{T(\phi)}$ is equal to 1). The periodic orbit is elliptic if the spectrum is $(e^{i\omega(\phi)}, e^{-i\omega(\phi)})$ (and stable, except at some particular values), or hyperbolic if the spectrum is $(\lambda(\phi), 1/\lambda(\phi))$ with $\lambda(\phi) \in \mathbb{R}^*$ (unstable). In a more concise form, it can be summarized using Greene's residue, R [23, 24]

$$R(\phi) = (2 - \text{tr}\mathcal{J}_\phi^{T(\phi)})/4.$$

If $R(\phi) \in]0, 1[$, the periodic orbit is elliptic; if $R(\phi) < 0$ or $R(\phi) > 1$ it is hyperbolic; and if $R(\phi) = 0$ and $R(\phi) = 1$, it is parabolic. Generically, periodic orbits and their linear stabilities are robust against small changes of parameters, except at specific values where bifurcations occur [25]. These rare events affect the dynamical behavior drastically.

In what follows, we identify the bifurcations (if any) of a set of short periodic orbits, i.e., the type and the value of the parameter ϕ_c where they bifurcate. This provides a way to foretell if a relatively high ionization rate should be expected or not. We use the residue curves $\phi \mapsto R(\phi)$ for each periodic orbit to analyze the dependence of ionization rates on ϕ . The importance of considering two associated Birkhoff periodic orbits (i.e. periodic orbits with the same action but different angles in the integrable case, one elliptic and one hyperbolic), was emphasized in Ref. [26]

Figure 1 shows a Poincaré section of Hamiltonian (2) for Case (I) at $\phi = 0$. We notice two main islands in the chaotic sea. At the centers of these islands sit elliptic periodic orbits with period 2π (indicated by full circles). Note that the (rescaled) principal quantum number considered in Ref. [20] lies in between these two islands. The residue method will monitor these two elliptic periodic orbits as well as their associated hyperbolic periodic orbits (they all have the same period $T(\phi) = 2\pi$ for all values of ϕ) [26]. We follow the location and residue for each of these periodic orbits as the parameter ϕ varies. Figure 2 shows the residue curves of these orbits.

In Fig. 2 (upper panel), if we start from $\phi = 0$ and follow the upper elliptic periodic orbit of Fig. 1, it remains elliptic ($R(\phi) \in]0, 1[$) until $\phi_c \approx 0.49$ where a bifurcation appears. At this critical value, the orbit is parabolic. Then it turns hyperbolic ($R(\phi) > 1$) until $2\pi/3 - \phi_c$ where another bifurcation occurs and the orbit returns to being

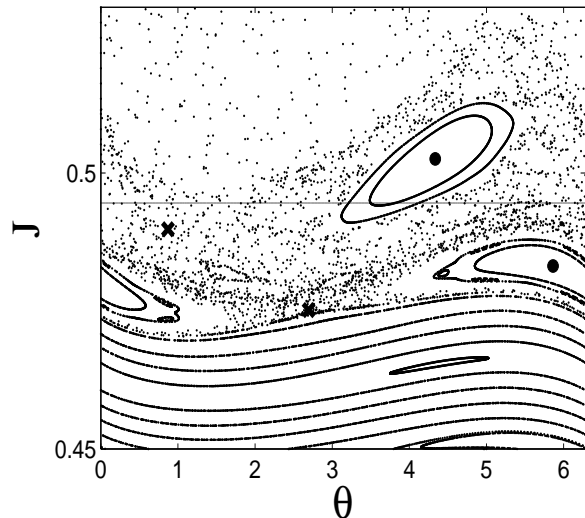


FIG. 1: Poincaré section of Hamiltonian (2) for Case (I) at $\phi = 0$. Full circles and crosses indicate the two elliptic and two hyperbolic periodic orbits we consider respectively. The horizontal line corresponds to the principal quantum number $n = 51$ considered in Ref. [20].

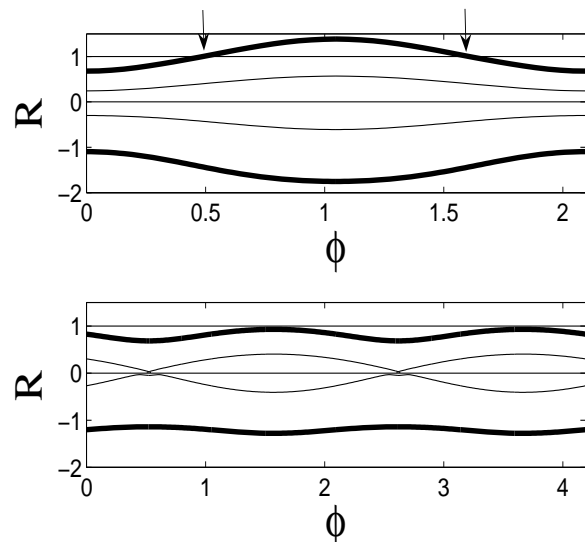


FIG. 2: Residue curves for the four periodic orbits with period 2π indicated by crosses and circles on Fig. 1. The bold curves are for the upper set of elliptic/hyperbolic orbits. Small arrows indicate where the bifurcations happen. Upper panel is for Case (I), i.e. $h:l=3:1$ and lower panel for Case (II), i.e. $h:l=3:2$.

elliptic. This bifurcation is of the period doubling kind at ϕ_c and a period halving one at $2\pi/3 - \phi_c$. The computation of $\log |\lambda_{\pm}(\phi)|$ (where $\lambda_{\pm}(\phi)$ are the two eigenvalues of the monodromy matrix $\mathcal{J}_\phi^{T(\phi)}$ associated with the upper elliptic periodic orbit) show that, before the bifurcation, $\log |\lambda(\phi)| = 0$ since the orbit is elliptic, and that

just after the bifurcation, $\log |\lambda_{\pm}(\phi)| \propto \pm \sqrt{\phi - \phi_c}$. Note that while the upper elliptic periodic orbit undergoes a bifurcation as ϕ is varied, the other three periodic orbits retain the stability properties they had at $\phi = 0$.

In the parameter range $\phi \in]\phi_c, 2\pi/3 - \phi_c[$, the upper part of phase space does exhibit more chaos. Since the initial atomic beam is taken in this region (principal quantum number $n = 51$ which corresponds to action $J_i \approx 0.495$), the ionization rate is expected to be higher in this regime. Apart from fine detail (like higher order islands), the upper part of phase space is roughly homogeneous. Therefore we expect to observe a plateau in the ionization probability versus ϕ . The reason is that a strongly hyperbolic orbit only influences the ionization time and not the value of the ionization probability. Of course, this is true provided that the duration of the maximum pulse envelope is large enough (in the experiment, this is approximately 15 times the period of the periodic orbits considered [20]). Roughly speaking, this means that in the chaotic region all the orbits ionize (i.e., escape to a value of the action $J_{\text{ion}} \gtrsim 1.26$) whatever the hyperbolicity degree is. In Ref. [20], experimental results as well as one-dimensional quantum calculations show this plateau. From quantum calculations, $\phi_c \approx 0.5$ was obtained in Ref. [20] which is in good agreement with the parameter value $\phi_c \approx 0.49$ at which the bifurcation of the upper elliptic periodic orbit occurs.

We perform the same analysis for Case (II) where $h:l=3:2$. Again we consider two main islands in the chaotic sea where two different elliptic periodic orbits with period 2π sit at the centers. We monitor the stability of four periodic orbits (two elliptic orbits and the associated hyperbolic ones). Figure 2 (lower panel) shows the four residue curves. Evidently the elliptic periodic orbits remain elliptic and the hyperbolic ones remain hyperbolic for all values of ϕ . No bifurcations occur; consequently, the ionization probability is expected to be approximately independent of ϕ and to be lower than Case (I) since for these values of amplitudes, the chaotic region is smaller. This is consistent with the experimental and quantum calculations of Ref. [20] (see their Fig. 7). The experimental results show a nearly flat curve for the ionization probability versus ϕ , whereas the quantum calculations show significant variations for this probability but no sharp increase and decrease as in Case (I).

The periodic orbit analysis above elucidates whether or not there is a significant ionization probability for specific parameter values, and also where plateaus are expected to occur. This qualitative agreement highlights the important role played by these orbits. Furthermore, we can obtain quantitative agreement concerning the shape of the ionization curve versus the phase ϕ by using the residue curves. To this end, we devise an empirical formula for relative ionization probability in the following way : First, the values of ϕ giving the highest ionization would be the ones associated with the highest variations of the residues (in absolute value) with respect to the minimum ionization. Second, if the periodic orbit is too

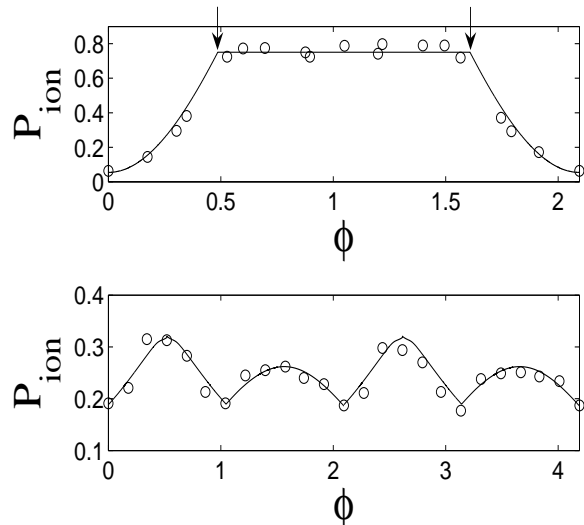


FIG. 3: Normalized ionization rate *vs* ϕ based on Eq. (3) for Case (I) (with $h:l=3:1$) with $A = -2.52$ and $B = 0.65$ (upper panel), and for Case (II) (with $h:l=3:2$) with $A = -0.485$ and $B = 0.17$. Circles represent the data obtained by one-dimensional quantum calculations, taken from Ref. [20].

far (in action) from the considered action J_i then it will not influence the dynamics so there should be a penalizing term depending on its position with respect to the chosen rescaled action. The formula reads :

$$P_{\text{ion}}(\phi) = A + B \sum_{m=1}^M \frac{\exp |R_m(\phi) - R_m(0)|}{\exp |\overline{J_m(\phi)} - J_i|}, \quad (3)$$

where the sum is taken over the M different periodic orbits considered and $\overline{J_m(\phi)} = \int_0^{2\pi} J(\theta) d\theta / 2\pi$ is the average action of the periodic orbit m . The parameters A and B in Eq. (3) are merely a translation and a dilatation of the curve in order to match the mean value and the amplitude of variations of P_{ion} obtained in Ref. [20]. This formula takes into account the value of the residues at $\phi = 0$. The aim is to set up a baseline for each of the periodic orbits (which is taken here at the value of the parameter where the ionization is minimal [20]). In general, Eq. (3) can exhibit values which are greater than 1, which are not relevant. In order to remedy to this problem, we truncate P_{ion} at the value where a bifurcation occurs. Therefore in the range where $R_n(\phi)$ is larger than one, P_{ion} is constant (taken as the value of the residue at ϕ_c where the bifurcation occurs).

Figure 3 depicts P_{ion} given by Eq. (3) versus parameter ϕ as well as the data taken from Ref. [20] for both cases [Case (I) (upper panel) and Case (II) (lower panel)]. Since there are no bifurcations in Case (II), there is no plateau. We notice that the empirical formula reproduces accurately the results obtained from quantum calculations. In particular, it captures some essential features of the ionization curve in Case (II), like the two unequal-

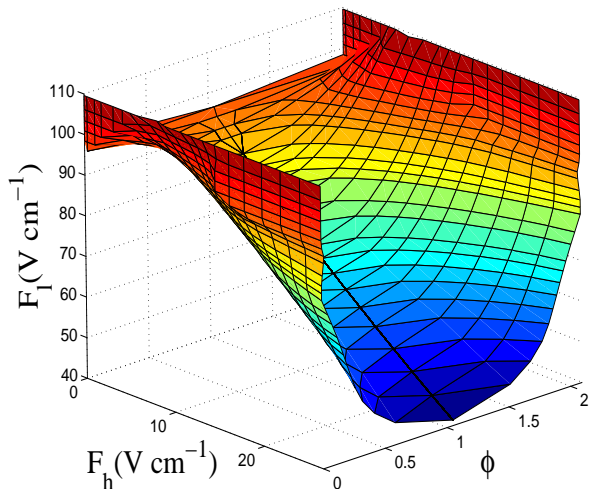


FIG. 4: Bifurcation surface in parameter space (ϕ, F_h, F_l) for $h:l=3:1$.

TABLE I: Ionization thresholds obtained for $F_h = 6 \text{ Vcm}^{-1}$, experimentally in Ref. [18] and by the residue method (see Fig. 4). The 1f case corresponds to $F_h = 0$.

$F_l (\text{Vcm}^{-1})$	$\phi = 0$	$\phi = \pi/3$	1f
[18]	107	85	96
residue	109.6	81.4	96.2

sized peaks and the specific shape of both peaks.

We can also predict the behavior of the system as all three parameters (the two amplitudes and the relative phase of the field) are varied. In Fig. 4, we represent the set of parameters where the upper elliptic periodic orbit of Fig. 1 (in the 3:1 case) is in fact parabolic (i.e., the set of parameters where the system undergoes a major bifurcation). The equation of this surface in parameter space is $R(\phi, F_h, F_l) = 1$. The boundaries of the plateaus in parameter ϕ of Fig. 3 (upper panel) obtained by fixing the two values for F_h and F_l are on this surface. We notice that as expected, when F_h approaches zero, this surface is less dependent on parameter ϕ . Table I compares the experimental values for ionization thresholds [18] with corresponding values from our bifurcation analysis.

To obtain this ionization surface in parameter space, a large number of classical trajectories for each value of the parameters (ϕ, F_h, F_l) needs to be computed for a sufficiently long time in order to decide whether or not a given trajectory has ionized. In contrast, only one orbit for a short time (typically the period of the field) is needed for the residue analysis. Furthermore, using residues, this surface can be constructed locally without any need to consider all possible values of the parameters.

More broadly, our results constitute rules by which this quantum system can be controlled. Such systematic and practical coherent control rules remain very rare and sought after [8].

This research was supported by the US National Science Foundation. C.C. acknowledges support from Euratom-CEA (contract EUR 344-88-1 FUA F).

-
- [1] P. Cvitanović, R. Artuso, R. Mainieri, G. Tanner and G. Vattay, *Chaos: Classical and Quantum*, ChaosBook.org (Niels Bohr Institute, Copenhagen 2005).
- [2] R. Blümel and W.P. Reinhardt, *Chaos in Atomic Physics* (Cambridge University Press, Cambridge, UK, 1997).
- [3] J.E. Bayfield and P.M. Koch, Phys. Rev. Lett. **33**, 258 (1974).
- [4] B.I. Meerson, E.A. Oks and P.V. Sasorov, Pis'ma Zh. Eksp. Teor. Fiz. **29**, 79 (1979) [JETP Lett. **29**, 72 (1979)].
- [5] G. Casati, B.V. Chirikov, I. Guarneri and D.L. Shepelyansky, Phys. Rep. **154**, 77 (1987).
- [6] R.V. Jensen, S.M. Susskind and M.M. Sanders, Phys. Rep. **201**, 1 (1991).
- [7] P.M. Koch and K.A.H. van Leeuwen, Phys. Rep. **255**, 289 (1995).
- [8] H. Rabitz, R. de Vivie-Riedle, M. Motzkus and K. Kompa, Science **288**, 824 (2000).
- [9] M. Shapiro and P. Brumer, Phys. Rep. **425**, 195 (2006).
- [10] L. Ko, M.W. Noel and T.F. Gallagher, J. Phys. B **32**, 3469 (1999).
- [11] F. Ehlotzky, Phys. Rep. **345**, 175 (2001).
- [12] J.E. Howard, Phys. Lett. A **156**, 286 (1991).
- [13] A. Haffmans, R. Blümel, P.M. Koch and L. Sirko, Phys. Rev. Lett. **73**, 248 (1994).
- [14] A. Buchleitner, D. Delande and J.-C. Gay, J. Opt. Soc. Am. B **12**, 505 (1995).
- [15] D. Petrosyan and P. Lambropoulos, Phys. Rev. Lett. **85**, 1843 (2000).
- [16] M. Ivanov, P.B. Corkum, T. Zuo and A.D. Bandrauk, Phys. Rev. Lett. **74**, 2933 (1995).
- [17] L. Sirko, S.A. Zelazny, and P.M. Koch, Phys. Rev. Lett. **87**, 043002 (2001).
- [18] L. Sirko and P.M. Koch, Phys. Rev. Lett. **89**, 274101 (2002).
- [19] V. Batista and P. Brumer, Phys. Rev. Lett. **89**, 143201 (2002).
- [20] P.M. Koch, S.A. Zelazny and L. Sirko, J. Phys. B **36**, 4755 (2003).
- [21] C. Rangan, A.M. Bloch, C. Monroe and P.H. Bucksbaum, Phys. Rev. Lett. **92**, 113004 (2004).
- [22] V. Constantoudis and C.A. Nicolaides, J. Chem. Phys. **122**, 084118 (2005).
- [23] J.M. Greene, J. Math. Phys. **20**, 1173 (1979).
- [24] R.S. MacKay, Nonlinearity **5**, 161 (1992).
- [25] J.R. Cary and J.D. Hanson, Phys. Fluids **29**, 2464 (1986).
- [26] R. Bachelard, C. Chandre and X. Leoncini, Chaos **16**, 023104 (2006).